EFFECT OF BEAM CHROMATICITY ON FOREGROUNDS IN WIDE-FIELD MEASUREMENTS OF REDSHIFTED 21 CM POWER SPECTRA

Nithyanandan Thyagarajan[1*], TBD

Draft version January 12, 2016

ABSTRACT

Keywords: cosmology: observations — dark ages, reionization, first stars — large-scale structure of universe — methods: statistical — radio continuum: galaxies — techniques: interferometric

1. INTRODUCTION

The period in the history of the Universe characterized by the transition of neutral hydrogen in the intergalactic medium (IGM) to a fully ionized state due to the formation of radiating objects such as the first stars and galaxies is referred to as the Epoch of Reionization (EoR). This is an important period of nonlinear growth of matter density perturbations and astrophysical evolution leading to the large scale structure observed currently in the Universe. And yet, this period in the Universe's history has remained poorly probed to date with observations.

The redshifted neutral hydrogen from the IGM in this epoch has been identified to be one of the most promising and direct probes of the EoR (Sunyaev & Zeldovich 1972; Scott & Rees 1990; Madau et al. 1997; Tozzi et al. 2000; Iliev et al. 2002). Numerous experiments using low frequency radio telescopes targeting the redshifted 21 cm line from the spin-flip transition of HI have become operational such as the Murchison Widefield Array (MWA; Lonsdale et al. 2009; Bowman et al. 2013; Tingay et al. 2013), the Precision Array for Probing the Epoch of Reionization (PAPER; Parsons et al. 2010), the Low Frequency Array (LOFAR; van Haarlem et al. 2013) and the Giant Metrewave Radio Telescope EoR experiment (GMRT; Paciga et al. 2013). These instruments have sufficient sensitivity for a statistical detection of the EoR signal via estimating the spatial power spectrum of the redshifted HI temperature fluctuations (Beardsley et al. 2013; Thyagarajan et al. 2013). These instruments are intended to be precursors and pathfinders to the next generation of low frequency radio observatories such as the Hydrogen Epoch of Reionization Array[3] (HERA; DeBoer et al. 2015) and the Square Kilometre Array[4] (SKA). These next-generation instruments will advance the capability from a mere statistical detection of the signal to a direct three-dimensional tomographic imaging of the HI during the EoR.

The most significant challenge to low frequency EoR observations arises from the extremely bright Galactic and extragalactic foreground synchrotron emission which are $\sim 10^4$ times stronger than the desired EoR signal (Di Matteo et al. 2002; Ali et al. 2008; Bernardi et al. 2009, 2010; Ghosh et al. 2012). All the current and future instruments rely on the inherent differences in spatial isotropy and spectral smoothness between the EoR signal and the foregrounds to extract the EoR power spectrum (see, e.g., Furlanetto & Briggs 2004; Morales & Hewitt 2004; Zaldarriaga et al. 2004; Santos et al. 2005; Furlanetto et al. 2006; McQuinn et al. 2006; Morales et al. 2006; Wang et al. 2006; Gleser et al. 2008).

When expressed in the coordinate system of power spectrum measurements described by the three-dimensional wavenumber (k), the foreground emission is restricted to a wedge-shaped region commonly referred to as the *foreground wedge* (Bowman et al. 2009; Liu et al. 2009, 2014a,b; Datta et al. 2010; Liu & Tegmark 2011; Ghosh et al. 2012; Morales et al. 2012; Parsons et al. 2012; Trott et al. 2012; Vedantham et al. 2012; Dillon et al. 2013; Pober et al. 2013; Thyagarajan et al. 2013; Dillon et al. 2014) whereas the EoR signal has spherical symmetry due to its isotropy which appears elongated along line of sight k modes due to peculiar velocity effects when dominated by matter density perturbations during early stages of reionization. The extreme dynamic range required to subtract foregrounds precisely demands high precision modeling of foregrounds as observed by modern wide-field instruments (Thyagarajan et al. 2015b,a).

2. THE HYDROGEN EPOCH OF REIONIZATION ARRAY

3. DELAY SPECTRUM

(Parsons et al. 2012)

3.1. *The Wide-Field "Pitchfork" Effect*

(Thyagarajan et al. 2015b,a)

4. SIMULATIONS

We describe the instrument and foreground models used in our simulations.

4.1. *Antenna Power Pattern*

(Neben et al. 2015)

4.2. *Foreground Model*

5. CHROMATICITY OF POWER PATTERN

5.1. *Directional Chromaticity*

5.2. *Effect on Delay Power Spectrum*

5.3. *Constraints on Antenna-to-Antenna Reflections*

Patra et al. 2015 (submitted), Ewall-Wice et al. 2015 (submitted)

---

[1] Arizona State University, School of Earth and Space Exploration, Tempe, AZ 85287, USA
[*] e-mail: t_nithyanandan@asu.edu
[3] http://reionization.org/
[4] https://www.skatelescope.org/

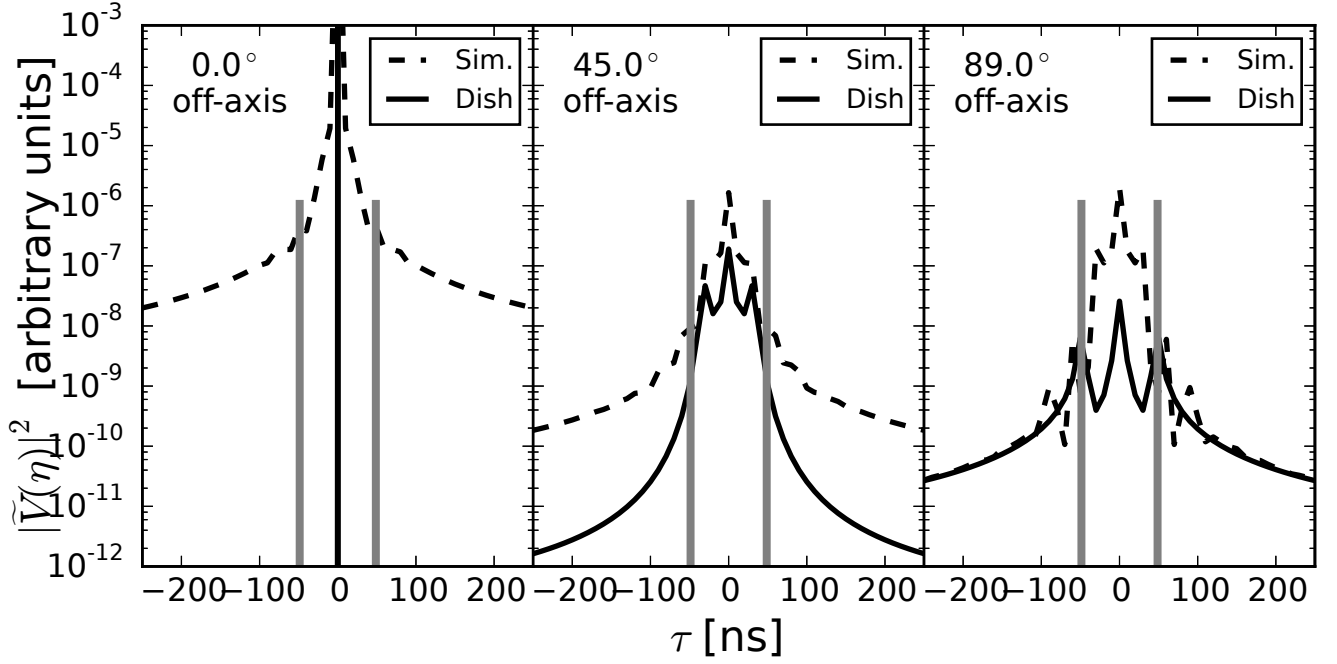**Figure 1.** Chromaticity of antenna power pattern at directions off-axis.
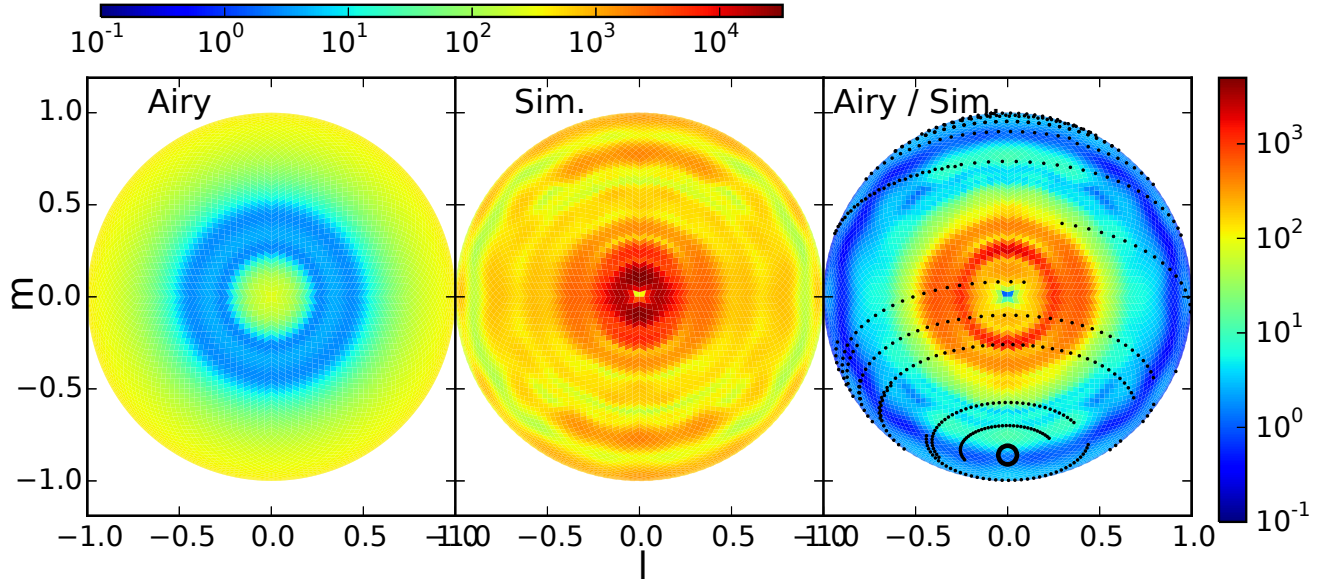
Figure 2. All-sky directional chromaticity of antenna power pattern.

6. SUMMARY

REFERENCES

Ali, S. S., Bharadwaj, S., & Chengalur, J. N. 2008, MNRAS, 385, 2166

Beardsley, A. P., Hazelton, B. J., Morales, M. F., et al. 2013, MNRAS, 429, L5

Bernardi, G., de Bruyn, A. G., Brentjens, M. A., et al. 2009, A&A, 500, 965

Bernardi, G., de Bruyn, A. G., Harker, G., et al. 2010, A&A, 522, A67

Bowman, J. D., Morales, M. F., & Hewitt, J. N. 2009, ApJ, 695, 183

Bowman, J. D., Cairns, I., Kaplan, D. L., et al. 2013, PASA, 30, 31

Datta, A., Bowman, J. D., & Carilli, C. L. 2010, ApJ, 724, 526

Di Matteo, T., Perna, R., Abel, T., & Rees, M. J. 2002, ApJ, 564, 576

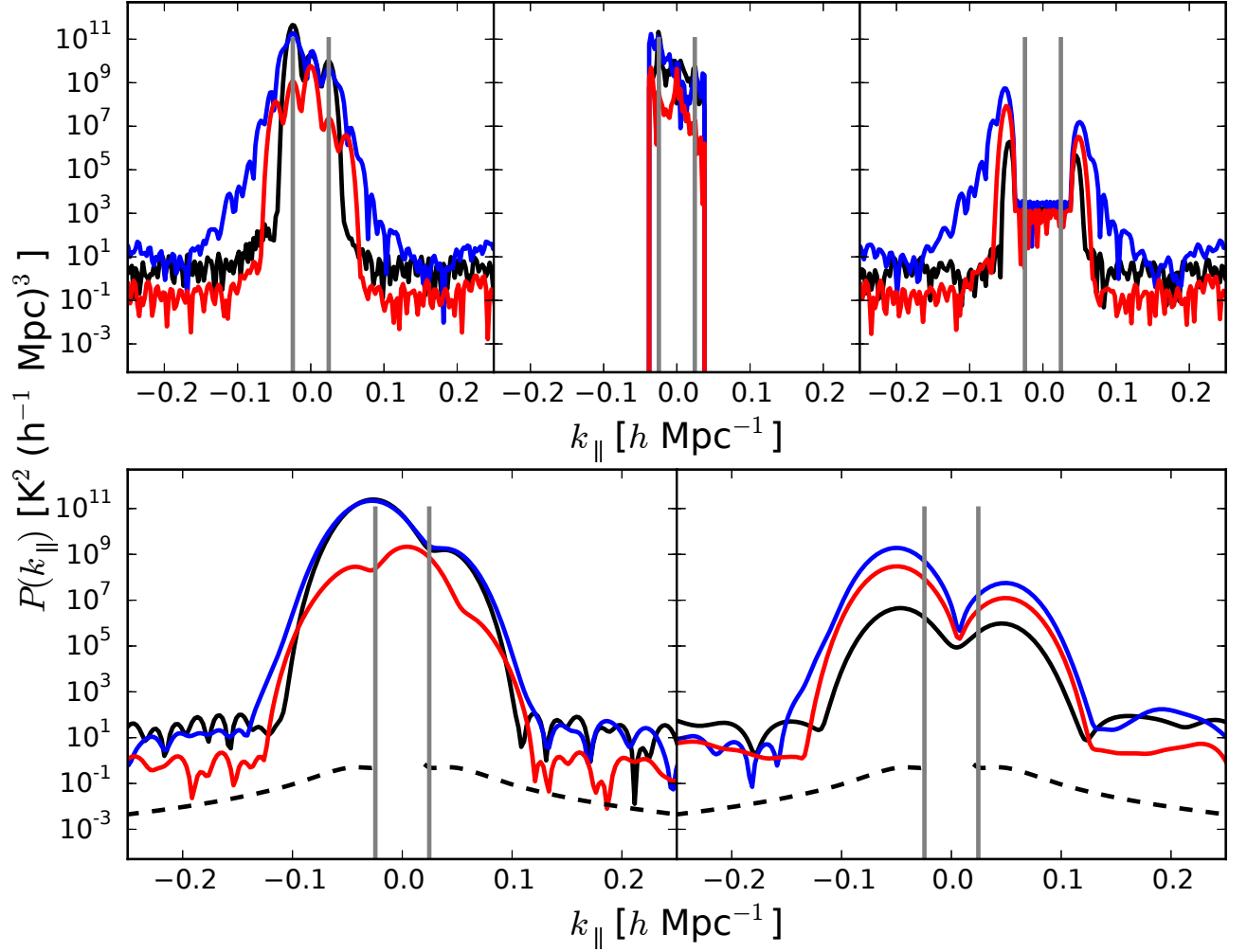Dillon, J. S., Liu, A., & Tegmark, M. 2013, Phys. Rev. D, 87, 043005

Figure 3. Effect of chromaticity of antenna power pattern on foreground delay power spectra.

Dillon, J. S., Liu, A., Williams, C. L., et al. 2014, Phys. Rev. D, 89, 023002

Furlanetto, S. R., & Briggs, F. H. 2004, New A Rev., 48, 1039

Furlanetto, S. R., Oh, S. P., & Briggs, F. H. 2006, Phys. Rep., 433, 181

Ghosh, A., Prasad, J., Bharadwaj, S., Ali, S. S., & Chengalur, J. N. 2012, MNRAS, 426, 3295

Gleser, L., Nusser, A., & Benson, A. J. 2008, MNRAS, 391, 383

Iliev, I. T., Shapiro, P. R., Ferrara, A., & Martel, H. 2002, ApJ, 572, L123

Liu, A., Parsons, A. R., & Trott, C. M. 2014a, Phys. Rev. D, 90, 023018

—. 2014b, Phys. Rev. D, 90, 023019

Liu, A., & Tegmark, M. 2011, Phys. Rev. D, 83, 103006

Liu, A., Tegmark, M., Bowman, J., Hewitt, J., & Zaldarriaga, M. 2009, MNRAS, 398, 401

Lonsdale, C. J., Cappallo, R. J., Morales, M. F., et al. 2009, IEEE Proceedings, 97, 1497

Madau, P., Meiksin, A., & Rees, M. J. 1997, ApJ, 475, 429

McQuinn, M., Zahn, O., Zaldarriaga, M., Hernquist, L., & Furlanetto, S. R. 2006, ApJ, 653, 815

Morales, M. F., Bowman, J. D., & Hewitt, J. N. 2006, ApJ, 648, 767

Morales, M. F., Hazelton, B., Sullivan, I., & Beardsley, A. 2012, ApJ, 752, 137

Morales, M. F., & Hewitt, J. 2004, ApJ, 615, 7

Neben, A. R., Bradley, R. F., Hewitt, J. N., et al. 2015, ArXiv e-prints, arXiv:1505.07114

Paciga, G., Albert, J. G., Bandura, K., et al. 2013, MNRAS, 433, 639

Parsons, A. R., Pober, J. C., Aguirre, J. E., et al. 2012, ApJ, 756, 165

Parsons, A. R., Backer, D. C., Foster, G. S., et al. 2010, AJ, 139, 1468

Pober, J. C., Parsons, A. R., Aguirre, J. E., et al. 2013, ApJ, 768, L36

Santos, M. G., Cooray, A., & Knox, L. 2005, ApJ, 625, 575

Scott, D., & Rees, M. J. 1990, MNRAS, 247, 510

Sunyaev, R. A., & Zeldovich, Y. B. 1972, A&A, 20, 189

Thyagarajan, N., Udaya Shankar, N., Subrahmanyan, R., et al. 2013, ApJ, 776, 6

Thyagarajan, N., Jacobs, D. C., Bowman, J. D., et al. 2015a, ApJ, 807, L28

—. 2015b, ApJ, 804, 14

Tingay, S. J., Goeke, R., Bowman, J. D., et al. 2013, PASA, 30, 7

Tozzi, P., Madau, P., Meiksin, A., & Rees, M. J. 2000, ApJ, 528, 597

Trott, C. M., Wayth, R. B., & Tingay, S. J. 2012, ApJ, 757, 101

van Haarlem, M. P., Wise, M. W., Gunst, A. W., et al. 2013, A&A, 556, A2

Vedantham, H., Udaya Shankar, N., & Subrahmanyan, R. 2012, ApJ, 745, 176

Wang, X., Tegmark, M., Santos, M. G., & Knox, L. 2006, ApJ, 650, 529

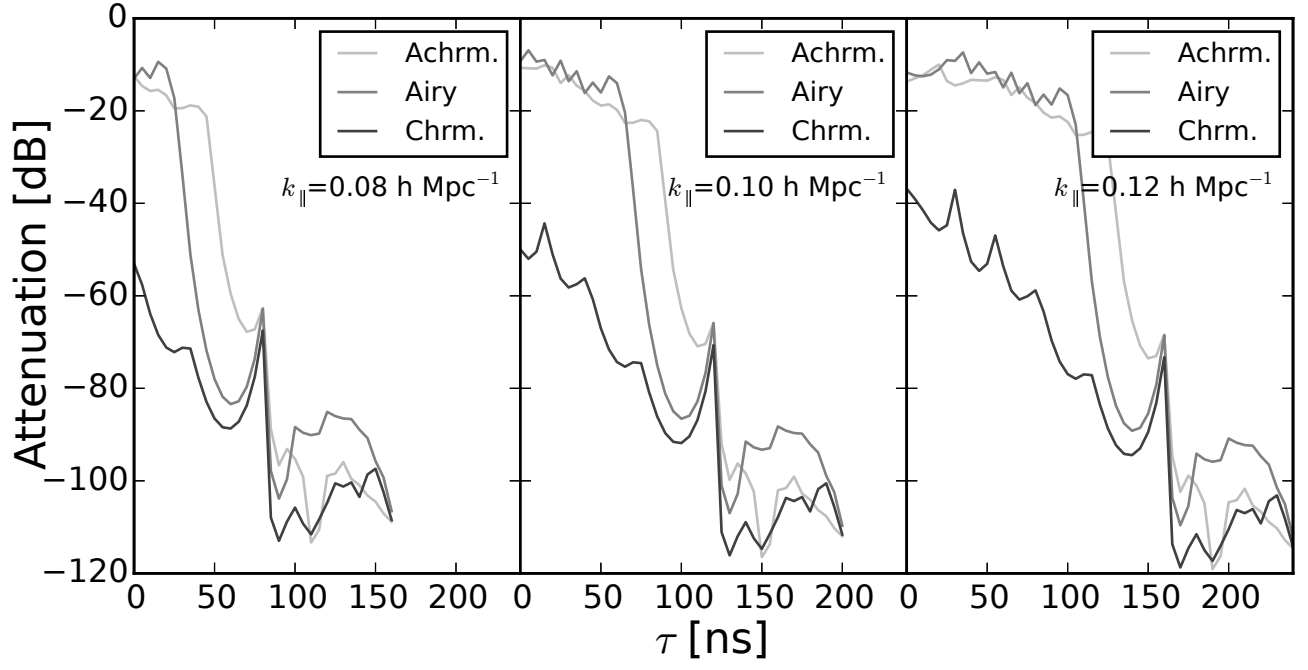Zaldarriaga, M., Furlanetto, S. R., & Hernquist, L. 2004, ApJ, 608, 622

Figure 4. Attenuation of foreground power (in dB) from antenna-to-antenna reflections required to keep the reflected foreground power below EoR H I signal power.